PHILOSOPHICAL MAGAZINE B, 1979, VOL. 39, NO. 5, 373–383

Phonon structure and proximity-effect tunnelling in strongly gapless superconductors

By B. F. DONOVAN-VOJTOVIC†, IVAN SCHULLER and P. M. CHAIKIN
Department of Physics, University of California, Los Angeles, California 90024, U.S.A.

[Received 31 August 1978 and accepted 16 January 1979]

ABSTRACT

The tunnelling characteristics of normal-metal–insulator–superconductor (NIS) and NINS junctions in the presence of a parallel magnetic field larger than the bulk critical field have been measured. The state that results from this surface superconductivity is gapless. By comparing data taken with no applied field and above H_{c_2}, we are able to study the strong coupling effects in a superconductor and the interference effects in a proximity sandwich as the order parameter is varied. In the case of the proximity effect, we are also able to obtain gaplessness by the addition of magnetic impurities to the normal metal N.

For tunnelling into a single superconducting film, the amplitude of the observed phonon structure scales with the order parameter squared. Although surface superconductivity is usually reduced by proximity with a normal metal, the surface sheath remains superconducting for a layer of silver up to ~800 Å thick for Ag–Pb sandwiches. For thin silver layers (~200 Å), the discrepancy between a simple interference model calculation and the experimental data becomes less as the order parameter is reduced, which implies that the discrepancy arises from multiple Andreev scatterings at the N–S boundary. A similar conclusion is reached from studies in which magnetic impurities are introduced into the normal metal.

§ 1. INTRODUCTION

Saint-James and de Gennes (1963) have shown that a superconductor can exhibit superconductivity on its surface while the bulk of the sample is in the normal state. By solving the linearized Landau–Ginsburg equation,

$$\frac{1}{2m}[i\hbar\nabla + (2eA/c)]^2\Psi = \alpha\Psi, \tag{1}$$

one can show that the eigenvalue solution corresponds to a critical field H_{c_2}. The superconductor is Type I if H_{c_2} is smaller than the thermodynamic critical field H_c, and Type II if it is greater. This, however, is valid only for an infinite sample where no boundary conditions need to be applied to eqn. (1). For a finite sample one must introduce the boundary condition $\partial\Psi/\partial x = 0$ if the superconductor's surface is in contact with a vacuum (de Gennes 1964). In this case there exists a lower eigenvalue solution to eqn. (1), corresponding to a higher critical field known as H_{c_3}. Thus, a finite superconductor will exhibit superconductivity on a surface sheath up to a critical field

† Present address: Instituto de Fisica, Unicamp, Campinas, São Paulo, 13100, Brazil.

$H_{c_3} = (1{\cdot}7 \pm 0{\cdot}05)H_{c_2}$ (Joiner and Blaugher 1964, Burger, Deutcher, Guyon and Martinet 1965). In a decreasing field the nucleation of the superconducting state is produced on the surface at H_{c_3} before being produced in the bulk at H_{c_2}. The ratio H_{c_3}/H_{c_2} is independent of the superconductor and of temperature (Burger 1965). Calculations show that the surface sheath extends into the material to a depth of approximately a coherence length.

Studies have shown that different experiments give different results for the value of the critical field (de Gennes 1964, Bon Mardion, Goodman and Lacaze 1964). Resistivity measurements show a higher critical field than do magnetization measurements which look only at superconductivity in the bulk of the sample. Surface impedance measurements (Cardona and Rosenblum 1964) as a function of d.c. magnetic field indicate that the quality of the surface may cause H_{c_3} to vary from $1{\cdot}4H_{c_2}$ to $1{\cdot}9H_{c_2}$.

In the present work fields between H_c (or H_{c_2}) and H_{c_3} are used to study the effects of gapless superconductivity on the electron tunnelling spectra of well-characterized superconducting and proximity-effect films. In particular, the tunnelling density of states is known to reflect the electron–phonon interaction by showing structure at the Van Hove singularities associated with different phonon modes. This study is aimed at determining how the phonon structure is modified when the material becomes gapless.

Phonon structure is also observed in proximity-effect junctions of the form metal–insulator–normal-metal–superconductor (MINS). Two effects are present in this case, ' strong coupling ' being responsible for the N layer phonon structure and an interference effect being responsible for the S layer structure. Previous experiments (Chaikin, Donovan-Vojtovic, Wilson and Deutcher 1977) have shown that a model developed by McMillan and Rowell (1969) adequately describes the interference structure for normal-metal thicknesses $d_N > 500$ Å. As we shall show, considerable deviations from this theory are observed for smaller values of d_N. The magnetic field and magnetic impurity doping experiments discussed in this paper were undertaken in order to understand why the model breaks down in the case of thin normal layers. We have also investigated the reduction of H_{c_3} with increasing thickness of the normal-metal layer.

§ 2. Sample preparation

The Al–oxide–Ag–Pb junctions were prepared by evaporating 3000 ± 300 Å of aluminium onto a microscope slide and edge-masking with ~ 800 Å of SiO_2. The tunnelling barrier was made by a glow-discharge technique similar to the one used by Miles and Smith (1963). After deposition, the aluminium film was exposed to 50 μm of dry oxygen for about 5 min. A current of about 5 mA was passed between an aluminium electrode, made of aluminium wire, and the metal mass of the evaporator. Care was taken to prevent the aluminium wire electrode from ' seeing ' the aluminium film. The electrode was circular in shape and located at an average distance of 2 cm from the glass substrate. After oxidation, a silver film was deposited, followed by 3000 ± 300 Å of either lead or a Pb–Bi alloy. For the preparation of $Ag_{1-x}Mn_x$ films, an alloy was formed in an arc furnace and then evaporated from an electron-beam gun. The concentration was determined from susceptibility measurements on

similarly prepared films (Schuller, Orbach, Fuller and Chaikin 1978). The Pb–Bi alloys were formed in the evaporation boat and the concentration determined by the weight of the initial constituents, the vapour pressures of lead and bismuth being similar.

§ 3. Phonon structure in a gapless superconductor

For tunnelling into a strong-coupling superconductor such as lead at energies above the energy gap, large deviations from the BCS electronic density of states are observed. These deviations occur at energies associated with the phonon frequencies of the material; here we take $\hbar\omega = eV$. For high bias voltages, the tunnelling density of states can be approximated by

$$N(\omega) = \omega/[\omega^2 - \Delta^2(\omega)]^{1/2} \simeq 1 + [\Delta^2(\omega)/2\omega^2], \tag{2}$$

where $\Delta(\omega)$ is the energy-dependent pair potential and must be self-consistently determined from the Eliashberg-gap equations. It has been shown that, as the applied parallel magnetic field approaches H_{c_3}, the Landau–Ginzburg order parameter at the surface of a 'dirty' superconductor varies as (Guyon, Martinet, Matricon and Pincus 1965)

$$|\Psi(x=0)|^2 \propto H_{c_3} - H, \tag{3}$$

and, since $\Psi \propto \overline{\Delta(\omega)}$ (Gorkov 1959, Caroli, de Gennes and Matricon 1963) one suspects that

$$|\Delta(\omega, x=0)|^2 \propto H_{c_3} - H. \tag{4}$$

The difference between the order parameter and the pair potential is that Ψ is a macroscopic—and therefore frequency-averaged—parameter, while $\Delta(\omega)$ is microscopic and its frequency dependence may change with the applied field. The exact nature of the frequency averaging may be obtained by comparing the strong coupling equation for $\Delta(\omega)$ (McMillan and Rowell 1969) with the simplified model used to calculate Ψ from $\Delta(\omega)$ given by Gorkov (1959) and Caroli *et al.* (1963) in which an average electron–phonon coupling constant and average pair amplitude are used instead of the Eliashberg-gap equations. We are thus testing whether $\Delta(\omega)$ scales with the order parameter at high frequencies, even when the superconductor is in the gapless regime.

The normalized density of states for a gapless superconductor is given (de Gennes 1966) by

$$N(\omega) \simeq 1 + \frac{\Delta_0}{2}\frac{\omega^2 - \Gamma^2}{(\omega^2 + \Gamma^2)^2}, \tag{5}$$

where Γ is a measure of the strength of the pair-breaking mechanism. Its magnitude depends on whether the mechanism is due to paramagnetic impurities or applied magnetic field. It is worth noting that the parameter Δ in eqn. (5) is usually derived for a gapless BCS superconductor, in which case Δ is independent of frequency. In the case of a strong coupling material we should write $\Delta(\omega)$ instead; however, since it is the low-frequency ($\Delta \sim \Gamma$) region that is usually of interest for this equation, we have inserted $\Delta_0 \equiv \Delta(\omega = 0)$, implying low frequency.

Fig. 1

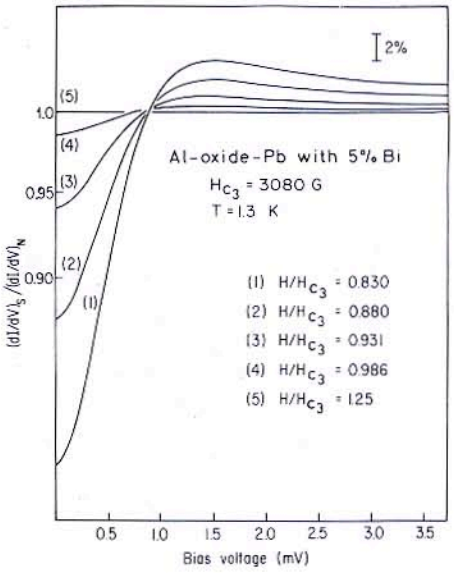

$(dI/dV)_S/(dI/dV)_N$ for Al–oxide–Pb with 5% bismuth in different parallel fields from 0 to 3·5 mV bias voltage.

Fig. 2

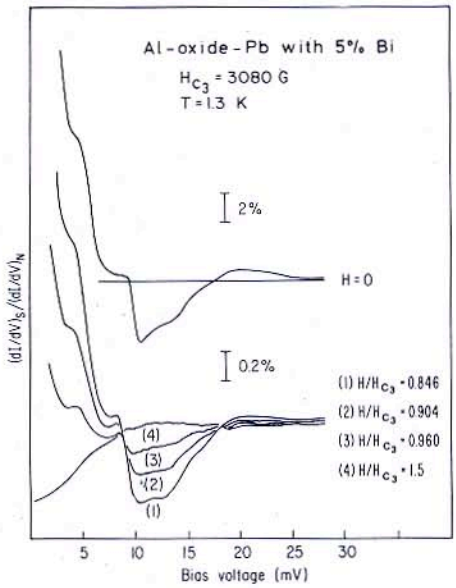

$(dI/dV)_S/(dI/dV)_N$ for Al–oxide–Pb with 5% bismuth from 5 to 25 mV bias voltage.

Figure 1 shows the first-derivative tunnelling characteristic dI/dV, which is proportional to the electronic density of states, of an Al–oxide–$Pb_{0\cdot96}Bi_{0\cdot04}$

junction, the bismuth being added to make the lead dirty. The resistance was measured with 50 μV modulation. Figure 1 shows the same signal taken in different parallel magnetic fields. H_{c_3} was found to be 3080 G by measuring the zero-bias conductance as a function of field.

Equation 5 adequately describes each tunnelling curve shown in fig. 1. We were therefore able to extract both Γ and Δ uniquely for each value of H/H_{c_3}. We find $\Gamma \sim 0{\cdot}89$ mV at H_{c_3}, and a linear variation of Δ^2 with $H_{c_3}-H$, in agreement with eqn. (4). Figure 2 shows the first-derivative characteristics at higher bias voltages in zero parallel field and for four different values of H/H_{c_3}. The structures around 6 mV and 10 mV correspond to the Van Hove singularities in the phonon density of states of lead (McMillan and Rowell 1969). It should be noted that the position of the structures has shifted by the value of the superconducting gap in going from the $H=0$ to the gapless regime. Figure 3 shows the second-harmonic signal of the same junction taken with a modulation voltage of 1 mV. One can see that the lead phonon structure is visible, even for a highly gapless sample. For clarity only one curve in the gapless region is shown.

Fig. 3

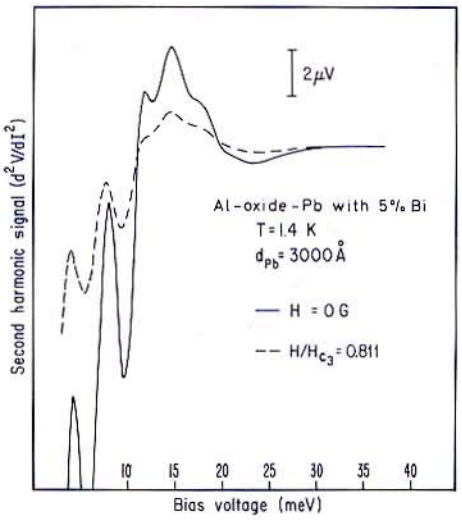

Second-harmonic signal of Al–oxide–Pb with 5% bismuth in zero field and $H/H_{c_3}=0{\cdot}811$.

Figure 4 shows a plot of the low-frequency pair potential Δ_0, the amplitude of the structure associated with the longitudinal acoustic phonon in lead at ~ 10 mV in dI/dV, and the same structure as observed in d^2V/dI^2 as a function of magnetic field. Δ_0 is determined from the tunnelling measurements around zero bias, as in fig. 1. The amplitude of the phonon structure is obtained from the deviation of the conductance from that in the normal state (see fig. 2 and eqn. (2)). The second-derivative structure is merely the size of the dips

at 10 mV in fig. 3 relative to a trace taken in the normal state. All these quantities have been normalized by their value obtained in zero field.

From fig. 4 we see that the high-frequency pair potential scales with the low-frequency pair potential, even for the transition from a well-defined gap to extreme gaplessness. The functional dependence on H is expected from eqn. (4). This indicates that the pair potential at all frequencies is related linearly to the order parameter.

Fig. 4

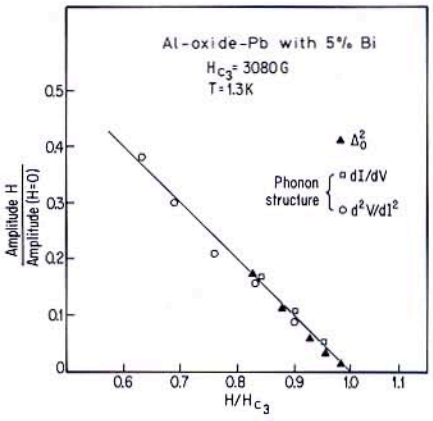

Δ_0^2, phonon structure in dI/dV and d^2V/dI^2 for different values of H/H_{c_3}.

It is interesting to note that Δ_0 must be determined in quite different ways in the two limits. With a well-defined gap, Δ_0 is equal to the gap, whereas in the extreme gapless limit, Δ_0 must be obtained from eqn. (5). For other values of applied fields, Δ_0 cannot be easily obtained from tunnelling measurements at low frequency. The phonon structure amplitude, however, is obtained in the same way in both limits. We would therefore suggest that the amplitudes of the phonon structure may be a good measure of the order parameter in all regions of fields, particularly in regions where it is otherwise inaccessible.

§ 4. Proximity-effect sandwiches

Shortly after the discovery of surface superconductivity, the suggestion was made that covering the superconductor with a normal metal would suppress the surface sheath. This question has been extensively investigated, both theoretically (Hurault 1966) and experimentally (Fisher and Klein 1966, Martinoli 1973, Tomasch 1964). While the primary concern of the work described in this section was the use of surface superconductivity to study the interference effect in a proximity-effect junction, we were also able to study the suppression of H_{c_3} with normal-metal thickness by tunnelling. This, surprisingly, is one surface superconductivity measurement that has not been exhaustively studied.

If the surface sheath is in contact with a normal metal, a current may flow through the interface. The new boundary condition to eqn. (1) may be written as $(1/\Psi)(\partial\Psi/\partial x) = 1/b$, where b is the extrapolation length in the normal metal and indicates a characteristic distance from the N–S interface at which the order parameter would go to zero in N if it were extrapolated linearly from the superconducting side (de Gennes 1964). The surface sheath is completely destroyed when a normal metal of infinite thickness is in contact with the superconductor (Hurault 1966), provided there is a good electrical contact between the two metals and the electrical conductivity in N is larger than the normal-state conductivity of S. Burger *et al.* (1965) have shown that no surface nucleation was possible for InBi–Zn junctions for which $\sigma_S/\sigma_N < 1$.

Care must be taken to avoid the formation of an oxide layer between N and S since the boundary condition depends on whether the superconductor is in contact with an insulator or a conductor. In our study of tunnelling characteristics of Al–oxide–Ag–Pb junctions, the silver film was deposited first in a vacuum of 10^{-5} Torr, the lead film being deposited a few seconds later. We have shown previously (Donovan-Vojtovic, Dodds and Chaikin 1978) that the time of evaporation between the silver and lead depositions was unimportant and did not change the second-derivative characteristics. The thickness of

Fig. 5

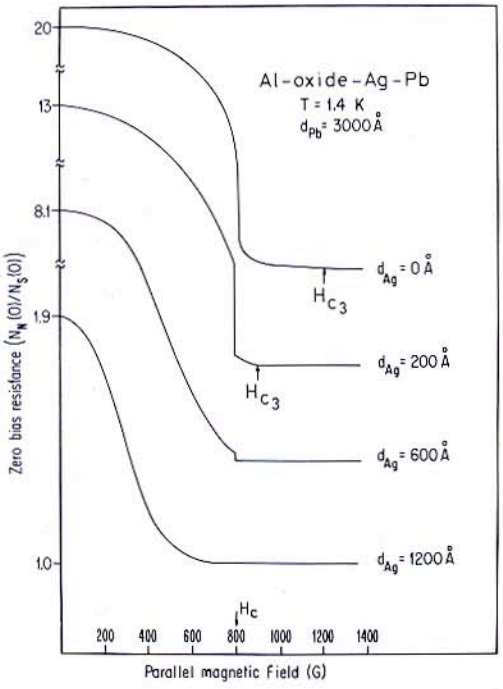

Zero-bias resistance ($N_N(0)/N_S(0)$) of an Al–oxide–Ag–Pb junction for silver layers 0, 200, 600 and 1200 Å thick. Vertical scales are linear with a different scale factor for each thickness. H_{c_3} for pure lead and a silver layer 200 Å thick are shown and were determined from an enlarged curve.

the silver film was varied from 50 to 1500 Å, the lead thickness being always 3000 Å.

Figure 5 shows the zero-bias resistance $N_N(0)/N_S(0)$ for an Al–oxide–Ag–Pb junction as a function of parallel magnetic field. The conductance *versus* voltage characteristics of our junctions are similar to those found by Adkins and Kington (1969). For the pure lead sample, both H_c ($\sim$800 G) and H_{c_3} ($\sim$1200 G) are clearly seen. For a thin normal layer of silver, for example one 200 Å thick, H_c is still seen at about 800 G, but H_{c_3} is diminished to about 900 G. For a thickness of 600 Å H_c is still visible, but H_{c_3} is barely visible, and for 1200 Å we see the destruction of superconductivity in N before H_c and thus see no H_{c_3}. From fig. 5 and other thickness studies we are able to determine H_{c_3} as a function of the normal-layer thickness ; the result is shown in fig. 6.

Fig. 6

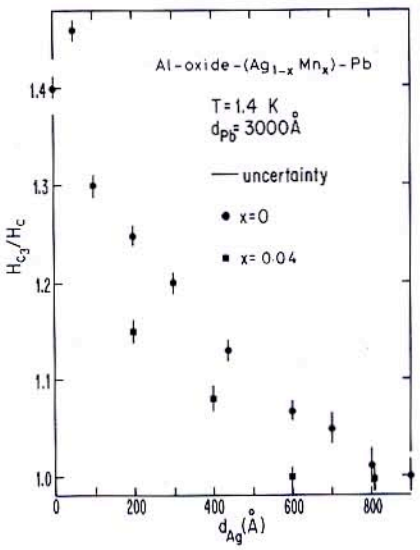

H_{c_3}/H_c versus d_{Ag} and manganese concentration.

H_{c_3}/H_c for pure lead is found to be $\sim$1·4, in good agreement with the measurements of Deutcher (1967). The 50 Å nominal thickness does not correspond to a continuous silver film ; the anomalous result may be due to a shortened mean free path (and hence coherence length) for electrons travelling parallel to the surface. One can see that surface superconductivity persists up to a normal-metal thickness of $\sim$800 Å for silver. From fig. 6 it is also seen that putting 0·4% of manganese in the silver film reduces H_{c_3}, but not dramatically.

Rowell and McMillan (1966) have shown that the tunnelling density of states for a proximity-effect sandwich contains a term that oscillates as a function of bias voltage because of electron-interference effects in the normal layer. This is due to the Andreev scattering of the electron wavefunction into a hole wavefunction by the pair potential Δ_{Pb} at the N–S interface. The scattered hole cannot interfere with the incident electron since it is in the normal metal. Thus one must wait until the hole is scattered at the oxide barrier and then

scattered back into an electron again at the N–S interface before interference may occur. The above theory involves a perturbative treatment of scattering and thus assumes Δ_{Pb} to be small. For this model the normalized density of states is

$$N(\omega) = 1 + \mathrm{Re}\left[\frac{{\Delta_{Pb}}^2}{2\omega^2}\tau^2 F\left(\frac{4d\omega}{\hbar V_F}\right)\right], \tag{6}$$

where

$$F(y) = \int_1^\infty x^{-2}\exp(ixy)\,dx, \tag{7}$$

V_F is the Fermi velocity in N, d the thickness of the normal metal and τ^2 the transmission coefficient. This model considers only two scatterings of the electron wavefunction at the interface, thus giving ${\Delta_{Pb}}^2$ in eqn. (6). Clearly the number of scatterings at the N–S interface which produce constructive interference will depend on the film thickness, the electron mean free path and the strength of Δ_{Pb} at the interface.

Fig. 7

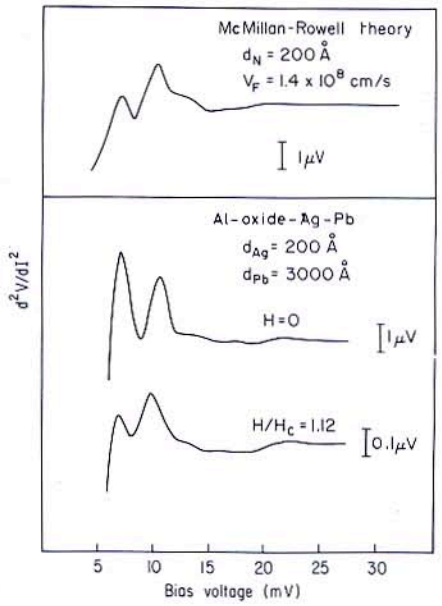

Theoretical and experimental curves of Al–oxide–Ag–Pb for $d_{Ag} = 200$ Å.

Figure 7 shows the second-derivative characteristics calculated from eqn. (6) for a normal layer of 200 Å and a Fermi velocity of $1{\cdot}4 \times 10^8$ cm/s, which was determined for silver from previous measurements (Donovan-Vojtovic *et al.* 1978). In addition it shows the experimental results for an Al–oxide–Ag–Pb junction with $d_{Ag} = 200$ Å. In zero magnetic field, both the amplitude and frequency dependence are seen to disagree with the theory. The first peak is higher than the second, whereas the opposite is true in the theoretical curve.

scattered back into an electron again at the N–S interface before interference may occur. The above theory involves a perturbative treatment of scattering and thus assumes Δ_{Pb} to be small. For this model the normalized density of states is

$$N(\omega) = 1 + \mathrm{Re}\left[\frac{{\Delta_{Pb}}^2}{2\omega^2}\,\tau^2 F\left(\frac{4d\omega}{\hbar V_F}\right)\right], \tag{6}$$

where

$$F(y) = \int_1^\infty x^{-2} \exp(ixy)\, dx, \tag{7}$$

V_F is the Fermi velocity in N, d the thickness of the normal metal and τ^2 the transmission coefficient. This model considers only two scatterings of the electron wavefunction at the interface, thus giving ${\Delta_{Pb}}^2$ in eqn. (6). Clearly the number of scatterings at the N–S interface which produce constructive interference will depend on the film thickness, the electron mean free path and the strength of Δ_{Pb} at the interface.

Fig. 7

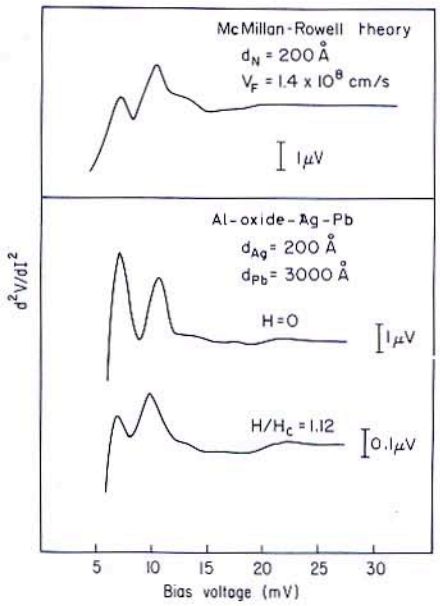

Theoretical and experimental curves of Al–oxide–Ag–Pb for $d_{Ag} = 200$ Å.

Figure 7 shows the second-derivative characteristics calculated from eqn. (6) for a normal layer of 200 Å and a Fermi velocity of $1{\cdot}4 \times 10^8$ cm/s, which was determined for silver from previous measurements (Donovan-Vojtovic *et al.* 1978). In addition it shows the experimental results for an Al–oxide–Ag–Pb junction with $d_{Ag} = 200$ Å. In zero magnetic field, both the amplitude and frequency dependence are seen to disagree with the theory. The first peak is higher than the second, whereas the opposite is true in the theoretical curve.

Several authors have noted this discrepancy in previous studies (So and Bermon 1978), the usual result being that normal-metal films about 200 Å thick or less appear to fit the Rowell–McMillan model, but only if physically unrealistic values of the Fermi velocity are chosen.

In a parallel field corresponding to $H/H_c \simeq 1{\cdot}12$, a qualitatively better agreement between theory and experiment is found. We suggest that the magnetic field has reduced Δ throughout the sandwich, particularly at the interface, thus the perturbation treatment which assumes Δ to be small is a better approximation in this case. Equation (6) should therefore be modified for thin normal metals to include multiple scattering at the N–S interface. Such a theory has recently been proposed by Arnold (1978).

Fig. 8

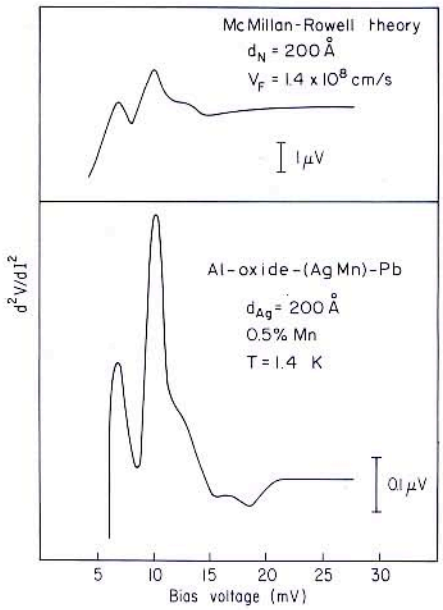

Theoretical and experimental curves of Al–oxide–Ag–Pb for $d_{Ag} = 200$ Å and 0·5% manganese.

In fig. 8 we have compared the McMillan–Rowell model with experiments on an (Ag, Mn)–Pb sandwich. The interference structure has been reduced, but we see striking similarity between the theoretical and experimental curves. The effect of the impurities in this case is twofold. First, they act as potential scattering sights which reduce the mean free path and hence limit multiple scatterings, whether they be normal or Andreev, and secondly they act as pair-breakers and lower Δ to reduce Andreev scattering further.

Since the effect of the magnetic impurities is similar to the effect of a magnetic field, we believe that the zero-field discrepancy with theory is largely due to the multiple Andreev scatterings which are taking place for large Δ.

§ 5. Conclusions

By using surface superconductivity as a means of producing gaplessness in otherwise unaltered tunnel junctions, we have found that :

(1) the phonon structure in the tunnelling characteristics scales with the order parameter and may provide an accurate way of determining the order parameter in regions where it is otherwise inaccessible,

(2) surface superconductivity persists for silver thicknesses up to 800 Å in Ag–Pb sandwiches, and

(3) proximity-effect sandwiches with thin normal metals exhibit interference effects with sizeable contribution from multiple scattering.

Acknowledgments

We should like to thank G. Deutcher and P. Pincus for interesting discussions, and Miss Cam Huong Nguyen and E. Chock for preparing some of the samples. The research was supported by ONR contract N0014–75–C–0245, and NSF grants DMR 76–82347 and DMR 78–12000.

References

Adkins, C. J., and Kington, B. W., 1969, *Phys. Rev.*, **177,** 777.
Arnold, G., 1978, *Phys. Rev.* B, **18,** 1076.
Bon Mardion, G., Goodman, B. B., and Lacaze, A., 1964, *Physics Lett.*, **8,** 15.
Burger, J. P., 1965, *J. Phys. appl., Paris*, **26,** 263.
Burger, J. P., Deutcher, G., Guyon, E., and Martinet, A., 1965, *Phys. Rev.*, **137,** 853.
Cardona, M., and Rosenblum, B., 1964, *Physics Lett.*, **8,** 308.
Caroli, C., de Gennes, P. G., and Matricon, J., 1963, *Phys. kondens. Mat.*, **1,** 176.
Chaikin, P. M., Donovan-Vojtovic, B. F., Wilson, J. A., and Deutcher, G., 1977, *Solid St. Commun.*, **21,** 331.
de Gennes, P. G., 1964, *Rev. mod. Phys.*, **36,** 225 ; 1966, *Superconductivity of Metals and Alloys* (New York : W. A. Benjamin, Inc.).
Deutcher, G., 1967, *J. Phys. Chem. Solids*, **28,** 741.
Donovan-Vojtovic, B. F., Dodds, S., and Chaikin, P. M., 1978, *J. Phys., Paris*, **39,** 521.
Fisher, G., and Klein, R., 1966, *Physics Lett.*, **23,** 311.
Gorkov, L. P., 1959, *Zh. éksp. teor. Fiz.*, **37,** 1407 (English translation : 1960, *Soviet Phys. JETP*, **10,** 998).
Guyon, E., Martinet, A., Matricon, J., and Pincus, P., 1965, *Phys. Rev.*, **138,** 746.
Hurault, J. P., 1966, *Physics Lett.*, **20,** 587.
Joiner, W. C. H., and Blaugher, R. D., 1964, *Rev. mod. Phys.*, **36,** 67.
McMillan, W. L., and Rowell, J. M., 1969, *Superconductivity*, edited by R. Parks (New York : Marcel Dekker), p. 561.
Martinoli, P., 1973, *Phys. kondens. Mat.*, **16,** 53.
Miles, J. L., and Smith, P. H., 1963, *J. electrochem. Soc.*, **110,** 1240.
Rowell, J. M., and McMillan, W. L., 1966, *Phys. Rev. Lett.*, **16,** 453.
Saint-James, D., and de Gennes, P. G., 1963, *Physics Lett.*, **7,** 306.
Schuller, I., Orbach, R., Fuller, W. W., and Chaikin, P. M., 1978, *Bull. Am. phys. Soc.*, **23,** 262.
So, C. K., and Bermon, S., 1978, *Bull. Am. phys. Soc.*, **23,** 263.
Tomasch, W. J., 1964, *Physics Lett.*, **9,** 104.